LAWRENCE
LIVERMORE
NATIONAL
LABORATORY

UCRL-PROC-201681

Effect of the environment and alloy composition on the electrochemical behavior of Ni-Cr-Mo Alloys

J. R. Hayes, A. W. Szmodis, K. L. Anderson, C. A. Orme

January 5, 2004

National Association of Corrosion Engineers
New Orleans, LA, United States
March 28, 2004 through April 1, 2004

UCRL-PROC-201681

EFFECT OF THE ENVIRONMENT AND ALLOY COMPOSITION ON THE ELECTROCHEMICAL BEHAVIOR OF Ni-Cr-Mo ALLOYS

Joel R. Hayes, Alan W. Szmodis, Kelly L. Anderson and Christine A. Orme
Lawrence Livermore National Laboratory, Livermore, CA 94550, USA

ABSTRACT

Alloy 22 (UNS N06022) is the candidate material for the corrosion resistant, outer barrier of the Yucca Mountain nuclear waste containers. One of the potential corrosion degradation modes of the container is uniform or passive corrosion. Therefore it is of importance to understand the stability of the oxide film, which will control the passive corrosion rate of Alloy 22. Many variables such as temperature, composition and pH of the electrolyte, applied potential, and microstructure and composition of the base metal would determine the thickness and composition of the oxide film. The purpose of this research work was to use electrochemical and surface analysis techniques to explore the influence of solution pH and applied potential on the characteristics of the oxide film formed on Alloy 22 and two experimental alloys containing differing amounts of chromium (Cr) and molybdenum (Mo). Results confirm that bulk metal composition is fundamental to the passive behavior and potential breakdown of the studied alloys. In these preliminary results, welded and non-welded Alloy 22 did not show differences in their anodic behavior.

Keywords: N06022, Ni-Cr-Mo alloys, general corrosion, pH, passive films

INTRODUCTION

Alloy 22 (UNS N06022), a highly corrosion resistant nickel based alloy, is currently considered as the corrosion barrier material for containers designed to store nuclear waste for up to 10,000 years in the United States. [1-3] The Yucca Mountain Project (YMP) plans to use this alloy as the outer layer of storage containers placed in a long term geologic nuclear waste storage facility bored deep into a mountain. Due to heat produced by the decay of radioactive isotopes, and the presence of salts deposited on the containers from water percolating through the surrounding rocks and from dust deposition, it is predicted that highly concentrated brines may eventually come into contact with the waste packages. This is expected to occur after the initial dry out stage of approximately 1000 years, the

time during which the drift temperature will be well above the boiling point of water. Thus, the corrosive behavior of the brines needs to be examined.

In order to understand and predict the corrosion rate and anodic behavior of Alloy 22, it is important to understand the behavior of the passive films formed on the materials surface when exposed to the predicted environments. The environment in the emplacement site is understood to be oxidizing (e.g. a water solution in contact with air). Chromium containing alloys such as N06022 rely on the integrity of a thin oxide film for protection against corrosion in oxidizing environments. The nature and thickness of the oxide film will strongly depend on environmental factors such as temperature, composition and pH of the electrolyte solution as well as on metallurgical factors such as uniformity of the composition of the beneficial alloying elements (e.g. Cr, Mo) and the possible presence of secondary phases at the weld seams. The composition of the oxide films that form on stainless alloys containing chromium depends largely on the pH of the solution. [4] A bilayer oxide film develops, with the inner layer (in contact with the alloy) richer in chromium than the outer layer (in contact with the electrolyte). [4] The effect of molybdenum (Mo) on the oxide film is not fully understood and it is still a matter of debate. [4] Several hypotheses were described on how Mo affects the passive film and decreases the susceptibility of the nickel and iron based stainless alloys to localized corrosion. [4] Kim et al. studied the oxide films formed on Alloy 22 when exposed to a saturated sulfate-chloride-nitrate-carbonate brine, pH 12.4 at 95°C for 2 months. [5] They used XPS analysis to measure the composition and thickness of the oxide film and reported that the surface film was 5 to 8 nm thick and was enriched in Cr. This film also contained Ni but the presence of Mo and W was not detected. Kim et al. also reported that the thickness of the oxide film formed on Alloy 22 did not vary significantly with the applied potential between –400 mV SCE and +200 mV SCE. [5] Szmodis et al. carried out cyclic polarization of Alloy 22 in more dilute brine solutions at pH 8 at 90°C. [6] They reported potentiodynamic polarization curves with two plateaus and an intermediate anodic peak between the plateaus. Using Atomic Force Microscopy (AFM) they reported obvious changes in the oxide film, especially at potentials above the anodic peak where the external layer becomes porous. X-ray photo electron spectroscopy (XPS) showed that the external layer contained mostly nickel oxide and iron oxide and the internal layer (near the base metal) contained oxides of all the major elements of Alloy 22, except tungsten. [6] Lloyd et al. studied the effect on the passive films formed on Alloys 22 and 276 when held potentiostatically at different temperatures. [7] They examined the films with XPS and Time-of-Flight Secondary Ion Mass Spectroscopy (TOF-SIMS). They found films consisting of Mo, Cr, and Ni oxide. The film on Alloy 22 displayed a layered structure, with a Cr and Ni rich inner layer and a Mo enriched outer layer.

Using thermodynamic data, it is possible to predict the stability of different phases, for example, in a domain of potential and pH (e.g a Pourbaix diagram) not only for pure elements and water but also for alloys in presence of aqueous solutions. This was done more or less in detail as a function of temperature for the nickel-chromium-iron system -and especially for Alloy 600 (N06600)- due to their importance in the nuclear power generation industry. [8-9] This has also been done recently for Alloy 22 (N06022) regarding its application for nuclear waste containment. [10]

Wrought plates of Alloy 22 are nickel based with the major alloying elements being 22% Cr, 13% Mo, 3% W and 3% Fe. Since the containers are going to be welded, some areas associated to the weld seam may contain a different proportion of alloying elements than the wrought base Alloy 22, for example in the interdendritic region.

In this study, nickel based alloys were tested electrochemically to determine their response to 1 M NaCl solutions buffered to various pH values. Three different nickel alloys were examined in order to test the

effects of the elements and elemental ratios within the alloy. The passive films resulting from the testing were examined with Auger Electron Spectroscopy (AES) and X-ray Photoelectron Spectroscopy (XPS) to determine their composition. These data will be compared against theoretical Pourbaix maps of alloys calculated using CALPHAD's Thermo-Calc software. [11] With these series of tests we hope to better understand the relationship between the passive film composition, the corrosive environment, and the corrosion behavior of the alloys. This paper discusses the results of the electrochemical studies. The passive film studies will be reported in a future paper.

EXPERIMENTAL

Metal Samples

Three alloy compositions were studied to examine the influence of specific elements and element ratios on the corrosion behavior of the alloys. The primary alloy studied is Alloy 22, a five-component alloy containing Ni, Cr, Mo, W, and Fe. Two types of Alloy 22 specimens were studied, mill annealed base metal and specimens containing a weld seam and the adjacent areas. The weld was produced by the gas tungsten arc welding (GTAW) using matching filler metal. This would allow the effect of the weld on the microstructure and alloy composition to be compared to that of the base metal. A ternary alloy designated Ni-11Cr-7Mo containing Ni, Cr, and Mo, and a binary alloy designated Ni-20Cr containing Ni and Cr were also studied. The weight percent composition of these alloys is detailed in Table 1. The samples were machined into 5/8" diameter discs 1/8" thick. A specimen number was inscribed on the back, and the front of the sample was mechanically polished by successively finer polishing compounds down to 0.02 µm colloidal silica. The exposed area of the disc during electrochemical testing was approximately 0.9 cm^2.

Solution Chemistries

A 1 M NaCl solution with 3 different pH values of 2.8, 7.5, and 11 were used to study how the alloys responded to changes in the pH of the testing electrolyte. The pH 2.8 solution contained 1 M NaCl, 0.07104 M of HCl, plus 0.1 M of the buffer KH-Phthalate. The pH 7.5 solution contained 1 M NaCl, 0.1 M Borate, and 0.02226 M NaOH. The pH 11 solution contained 1 M NaCl and 0.15 M NaOH. All of these solutions were tailored to maintain the designated pH level at a temperature of 90°C, the temperature at which all electrochemical experiments were performed.

Electrochemical Tests

The electrochemical tests were performed in a round bottom flask placed in a hot silicone oil bath. The bath was held at a temperature such that the electrolyte solution maintained a temperature of 90°C. A volume of 900 ml of solution was placed in the flask, and connected to the flask were ports containing the follow devices: A nitrogen bubbler flowing 99.999% pure N_2 gas was used to partially deareate the solution. A condenser tube connected to a chilled water line held at 15°C prevented evaporation of the electrolyte. A Luggin probe salt bridge connected a saturated Ag/AgCl (SSC) reference electrode to the electrolyte. All potential values are referenced to the Ag/AgCl reference electrode. A platinum counter electrode consisting of a platinum wire spot-welded to a 2 x 7 cm platinum foil flag was placed in front of the specimen, approximately 3 centimeters away from the specimen surface. The specimens were held in a vertical position to prevent corrosion products from settling on the surface, and to try to

minimize the diffusion depleted region in front of the sample through convection of the electrolyte. The Luggin probe tip was placed approximately 5 mm from the surface of the specimen.

A series of electrochemical tests were performed. The solution was placed in the flask, the temperature raised to 90°C, and then the solution was deaerated with N_2 for 1 hr. before the sample was placed into the solution. Before the sample was loaded, temperature and pH values were recorded. The sample was then inserted and the open circuit potential or corrosion potential (E_{corr}) was monitored for 24 hours. All electrochemical measurements were performed using a commercial potentiostat / galvanostat / zero resistance ammeter (ZRA). After the 24 hour period, a polarization resistance scan was performed according to ASTM G 102-89. These two steps were done on all samples. Current was recorded as the potential was stepped from 20 mV below, to 20 mV above the instantaneous E_{corr}, at a rate of 0.1667 mV/sec. The slope of this line, $\frac{\Delta V}{\Delta I}$, yields R_P, the polarization resistance.

After these two tests, one of two other tests were performed: a cyclic polarization, or the sample was held potentiostatically for 60,000 seconds (~ 17 h) at preselected potentials. The cyclic polarization scans were performed to examine the passive and breakdown behavior of the alloy. The cyclic polarization scans were run from 200 mV below the instantaneous E_{corr} up to 5 mA or 2000 mV vs. Ag/AgCl. The voltage was then stepped back to the original E_{corr} value. A scan rate of 0.1667 mV/sec was used. The surface morphology of these samples was examined optically in order to discern any localized corrosion. Several potentials were examined in each solution by holding a sample at a specified potential for 60,000 sec. The samples were then removed and the surface was studied with one or more of the following techniques: Atomic Force Microscopy (AFM), used to study the surface morphology and evolution of the passive film. AES depth profiling revealed the elements present as a function of depth in the oxide and the relative thicknesses of the oxides. XPS was used to examine the nature of the oxide bonding at the near surface of the passive layer. It can be used to look at the oxidation states of the elements in the film. These results will be presented in a future paper.

RESULTS AND DISCUSSION

Polarization Resistance (PR) and Corrosion Rates (CR)

The polarization resistance Rp is related to the corrosion rate by the equation [12]

$$R_P = \frac{B}{i_{corr}} \tag{1}$$

where i_{corr} is the corrosion current at which the cathodic and anodic reaction rates are equal, and B is related to the Tafel constants by:

$$B = \frac{\beta_a \beta_c}{2.3(\beta_a + \beta_c)} \tag{2}$$

Where β_a is the anodic Tafel constant and β_c is the cathodic Tafel constant

From Equation 1, i_{corr} can be calculated and used in the equation

$$r = \frac{kAi_{corr}}{EW \cdot D} \tag{3}$$

where k is a conversion constant, A is the specimen area, EW is the equivalent weight, and D is the density of the alloy. This will yield a general corrosion rate for the alloy/electrolyte system. A k value

of 3.27 μm/yr was used to yield a corrosion rate in units of μm/yr. Tables 1 and 2 list the values used for β_a, β_c, D, and EW for the alloys studied. β_a and β_c values were calculated from Tafel extrapolation of the cyclic polarization curves, when possible. When this was not possible a value of 0.12 V was used. The density of Alloy 22 is 8.69 g/cm³, the density of Ni-20Cr and Ni-11Cr-7Mo were calculate from a weighted average of the densities of their constituent elements. The equivalent weights for all alloys were calculated from a weighted average of the most common ionization states of their constituent elements (ASTM G 102). A summary of the corrosion rates calculated from the R_P data can be seen in Figure 1. In general the corrosion rates for all the studied pH and alloy compositions was very low (less than 3 μm/year), especially considering that the specimens were allowed to passivate for only 24 h. The corrosion rates of the alloys followed the general trend in which the higher rates were observed at pH 2.8, they decreased for pH 7.5 and slightly increased again for pH 11. Solutions with pH 7.5 always produced the lowest corrosion rates in all the studied alloys (Base Alloy 22, Welded Alloy 22, Ni-11Cr-7Mo and Ni-20Cr). A clear correlation between alloy composition and corrosion rate for the three studied pH values was not obvious. It is likely that for pH lower than 3, the effect of Mo on the corrosion rate would be more noticeable. For the studied pH values (2.8 to 11) and for the testing time involved, it is expected that the corrosion rate would be mostly controlled by the content of Cr in the alloys. Therefore, the overall corrosion rate at the three pH values was the highest for Ni-11Cr-7Mo alloy since it had only 11% Cr. The fact that the corrosion rate of Alloy 22 base metal in pH 2.8 solution was approximately double than the corrosion rate of welded Alloy 22 in the same tested conditions could be result of uncertainty. For the tested conditions there is not expected to be any difference in the corrosion behavior of these two materials.

Cyclic Potentiodynamic Polarization (CPP)

Cyclic polarization scans were performed according to ASTM G 61 on all alloys considered after a 24 hour E_{corr} stabilization. The passive region, the susceptibility to localized corrosion, and the repassivation potential can all be determined from a cyclic polarization curve. The cyclic polarization curves for 3 alloys in 1 M NaCl pH 2.8 can be seen in Figure 2. Note that only the base metal for Alloy 22 is shown, and not for the welded material. This was left out of this figure and each succeeding figure for simplicity. In all environments the base metal and weld metal cyclic polarization curves were practically identical. In the pH 2.8 solution, Alloy 22 had the largest passive region of nearly 1000 mV. Practically no hysteresis was observed, with a repassivation potential nearly the same as the breakdown potential of approximately 670 mV SSC. After repassivation the alloy displayed a sharp cathodic reduction peak near 550 mV, before returning to passive behavior. The Ni-11Cr-7Mo alloy had nearly the same passive region of almost 900 mV, yet metastable pitting initiated at 350 mV SSC. Severe localized corrosion occurred, and the surface did not repassivate until –300 mV was reached. The Ni-20Cr alloy also had localized corrosion initiating near 400 mV SSC, and the sample did not repassivate down to its initial E_{corr} value. These results show that an alloy containing only 11% Cr (Ni-11Cr-7Mo) was slightly more resistant to localized corrosion than an alloy containing 20% Cr (Ni-20Cr), obviously due to the 7% content of Mo in the former. That is, both elements Cr and Mo should be present simultaneously in the alloy for protection and more of one element does not substitute for the other.

The cyclic polarization curves of the 3 alloys in 1 M NaCl pH 7.5 can be seen in Figure 3. The passive region was not as distinctive in this mid-level pH solution. That is, the current in the passive region was practically independent of the applied potential in the pH 2.8 solution but it was a function of the applied potential in the pH 7.5 solution. Alloy 22 displayed an anodic peak at approximately 400 mV SSC, where the current rose sharply, then dropped back over a range of almost two orders of magnitude.

Some hysteresis occurred before the system repassivated at near 400 mV SSC. The ternary Ni-11Cr-7Mo sample showed pitting behavior, and had abrupt breakdown at 85 mV SSC, repassivating only when the potential reached –350 mV SSC. The binary Ni-20Cr sample did not have a marked passive region, and once breakdown occurred, it did not repassivate, similar to in the pH 2.8 solution. These three curves show again the importance of the balanced proportion of beneficial alloying elements in Alloy 22.

The cyclic polarization curves of the 3 alloys in 1 M NaCl pH 11, displayed in Figure 4, had the most complex behavior. Alloy 22 showed very little hysteresis, and once repassivation occurred, displayed 3 distinct cathodic reduction peaks, at 40, 270, and 360 mV SSC. The ternary Ni-11Cr-7Mo sample showed the largest passive range, and also had little hysteresis. After repassivation, it displayed 2 cathodic reduction peaks at 230 and 400 mV SSC. The binary Ni-20Cr had nearly the same initial passive behavior as Alloy 22, and after breakdown showed little hysteresis until the current dropped to 1 mA/cm^2, at which point significant hysteresis occurred. In alkaline solutions such as 1 M NaCl pH 11, the anodic behavior should be mostly controlled by nickel and NiO since this oxide is less soluble in alkaline solutions than either Cr_2O_3 and MoO_2 oxides. Mo and Cr are not beneficial elements for passivity in alkaline environments. The curves in Figure 4 show that Mo may still be controlling the occurrence of localized corrosion, where localized acidification is expected to occur. Figure 5 shows the polarization curves of the pure elements from Alloy 22 in 1 M NaCl solution of pH 11. Figure 5 shows that Ni offers the highest stability under these conditions. On the other hand, Mo and W offer poor resistance to anodic polarization in alkaline environments.

CONCLUSIONS

(1) The behavior of mill annealed (MA) and welded Alloy 22 were undistinguishable when polarized anodically in 1 M NaCl solution of pH 2.8, 7.5 and 11 at 90°C.

(2) The corrosion rate of Alloy 22 and two experimental Ni base alloys seemed to be a weak function of the solution pH. It was the highest at pH 2.8, decreased to a minimum at pH 7.5 and slightly increased at pH 11.

(3) For Alloys 22, Ni-11Cr-7Mo and Ni-20Cr, the most stable passivity was obtained in pH 2.8 solutions. Alloy 22 was free from localized attack after cyclic polarization but the other two alloys suffered pitting corrosion. The lowest resistance to localized corrosion was by Ni-20Cr.

(4) The passivity and composition of the oxide film of the three studied nickel alloys are a strong function of the solubility of the metal oxides at the tested solution pHs.

ACKNOWLEDGMENTS

This work was performed under the auspices of the U. S. Department of Energy (DOE) by the University of California Lawrence Livermore National Laboratory under contract N° W-7405-Eng-48. This work is supported by the Yucca Mountain Project, LLNL; which is part of the Office of Civilian Radioactive Waste Management (OCRWM), DOE.

REFERENCES

1. Yucca Mountain Science and Engineering Report, U. S. Department of Energy, Office of Civilian Radioactive Waste Management, DOE/RW-0539, Las Vegas, NV, May 2001.
2. G. A. Cragnolino, D. S. Dunn and Y.-M. Pan in Scientific Basis for Nuclear Waste Management XXV, Vol. 713, pp. 53-60 (Warrendale, PA: Materials Research Society 2002).
3. G. M. Gordon, Corrosion, 58, 811 (2002)
4. P. Marcus and V. Maurice "Passivity of Metals and Alloys" in Corrosion and Environmental Degradation, Volume I, p. 131 (Weinheim, Germany: Wiley-VCH 2000).
5. Y.-J. Kim, P. A. Andresen, P. J. Martiniano, J. Chera, M. Larsen and G. M. Gordon, Corrosion/2002, Paper 02544 (Houston, TX: NACE International, 2002)
6. A. W. Szmodis, K. L Anderson, J. C. Farmer, T. Lian and C. A. Orme, Corrosion/2003, Paper 03692 (Houston, TX: NACE International, 2003).
7. A.C. Lloyd, D.W. Shoesmith, N.S. McIntyre, and J.J. Noël, *J. Elec. Soc.*, **150** (4) B120 (2003).
8. C. M. Chen, K. Aral and G. J. Theus "Computer-Calculated Potential pH Diagrams to 300°C", NP-3137 (Palo Alto, CA: Electric Power Research Institute, 1983).
9. D. Cubicciotti, J. Nuclear Mater., 201, 176 (1993).
10. L. Kaufman, "Calculation of Pourbaix Diagrams for C-22 in Various Water Chemistries" Workshop on Fabrication, Welding and Corrosion of Nickel Alloys and Other Materials for Radioactive Waste Containers, Las Vegas, NV 16-17 October 2002 (Nickel Development Institute, 2002).
11. The Thermo-Calc applications softwares are products of Thermo-Calc AB; B. Sundman, B. Jansson, and J.-O. Andersson, CALPHAD **9** (4), 153 (1985).
12. D.A. Jones, *Principles and Prevention of Corrosion 2nd ed.*, Prentice Hall, New Jersey (1996).

Table 1: Composition of the 3 alloys tested with their density D and equivalent weight EW.

Alloy	Ni (w%)	Cr (w%)	Mo (w%)	W (w%)	Fe (w%)	D (g/cm^3)	EW
Alloy 22	59	22	13	3	3	8.69	23.28
Ni-11Cr-7Mo	82	11	7	0	0	8.75	25.86
Ni-20Cr	80	20	0	0	0	8.57	25.77

Table 2: Alloy Tafel constants calculated from cyclic potentiodynamic polarization. Values of 0.12 V were used when values could not be calculated.

	β_a (V)			β_c (V)		
Alloy	pH 2.8	pH 7.5	pH 11	pH 2.8	pH 7.5	pH 11
Alloy 22	0.29	0.17	0.28	0.25	0.14	0.27
Weld	0.12	0.19	0.12	0.12	0.12	0.12
Ni-11Cr-7Mo	0.12	0.15	0.31	0.12	0.08	0.17
Ni-20Cr	0.13	0.18	0.26	0.11	0.17	0.19

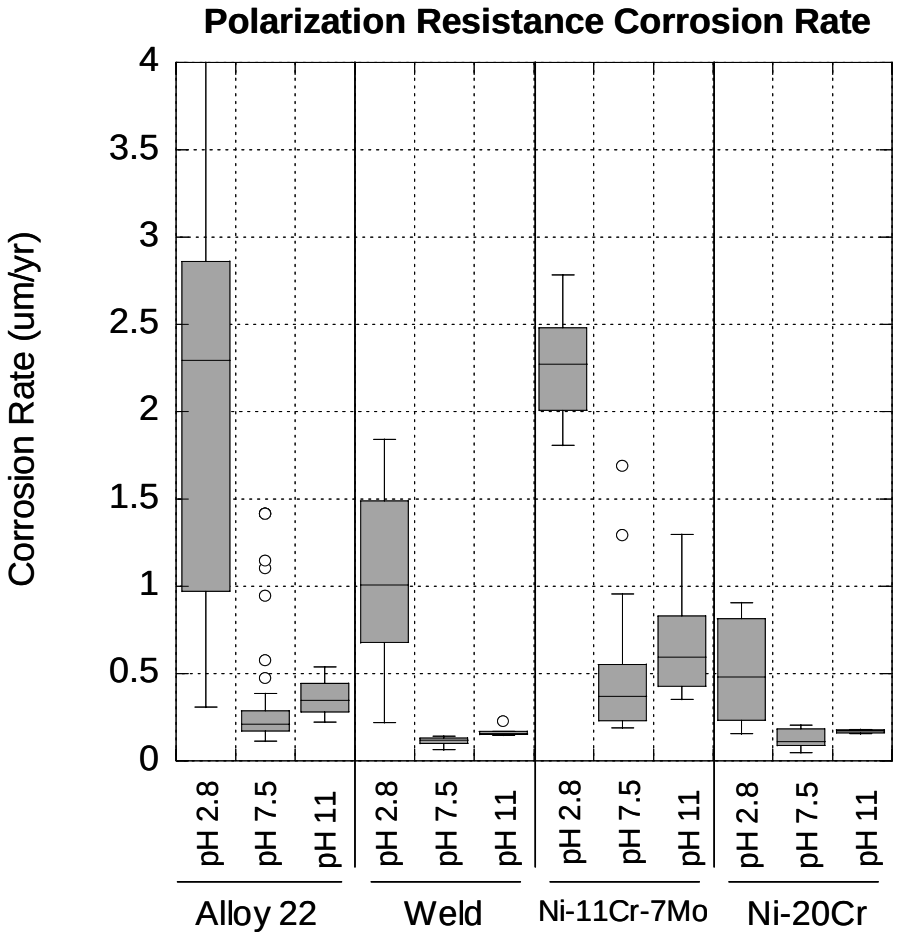

Figure 1: Corrosion rates of 4 types of samples in 3 solution chemistries calculated from polarization resistance curves.

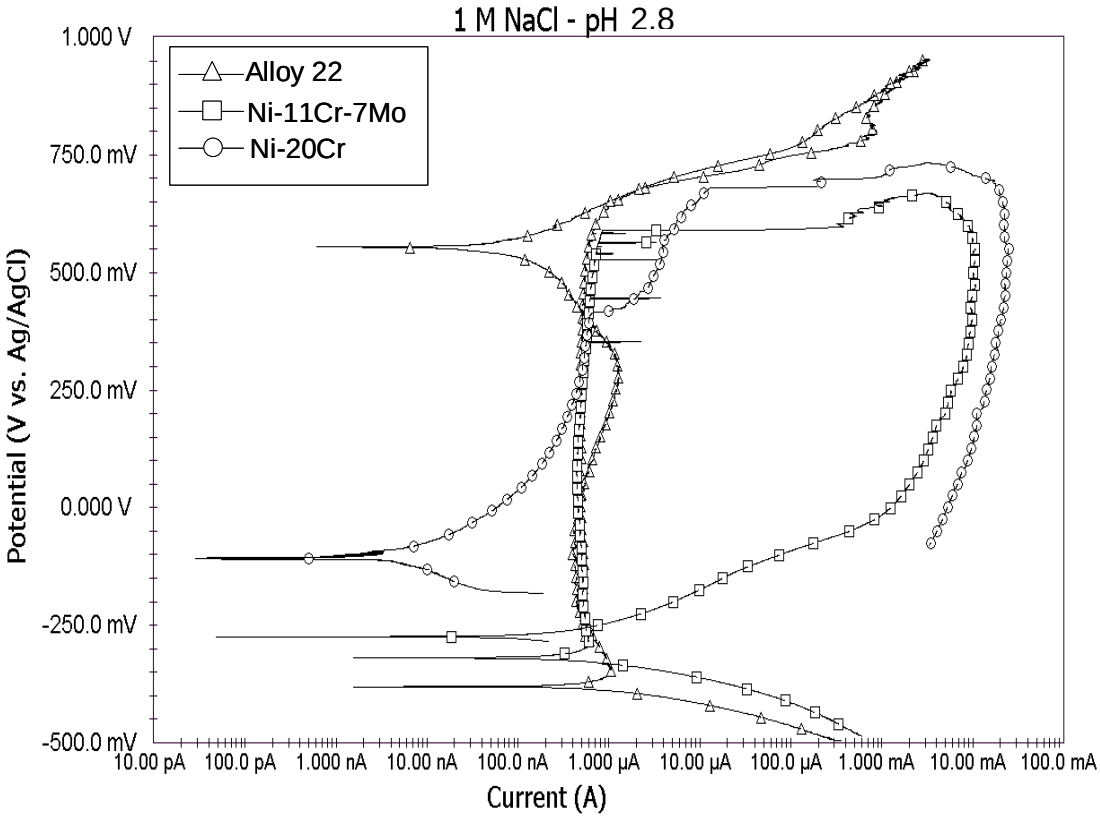

Figure 2: Cyclic potentiodynamic polarization of 3 alloys in 1 M NaCl solution at pH 2.8.

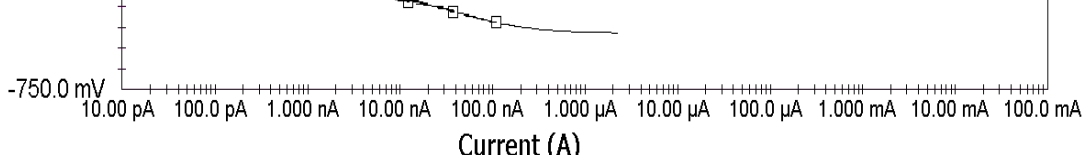

Figure 3: Cyclic potentiodynamic polarization of 3 alloys in 1 M NaCl solution at pH 7.5.

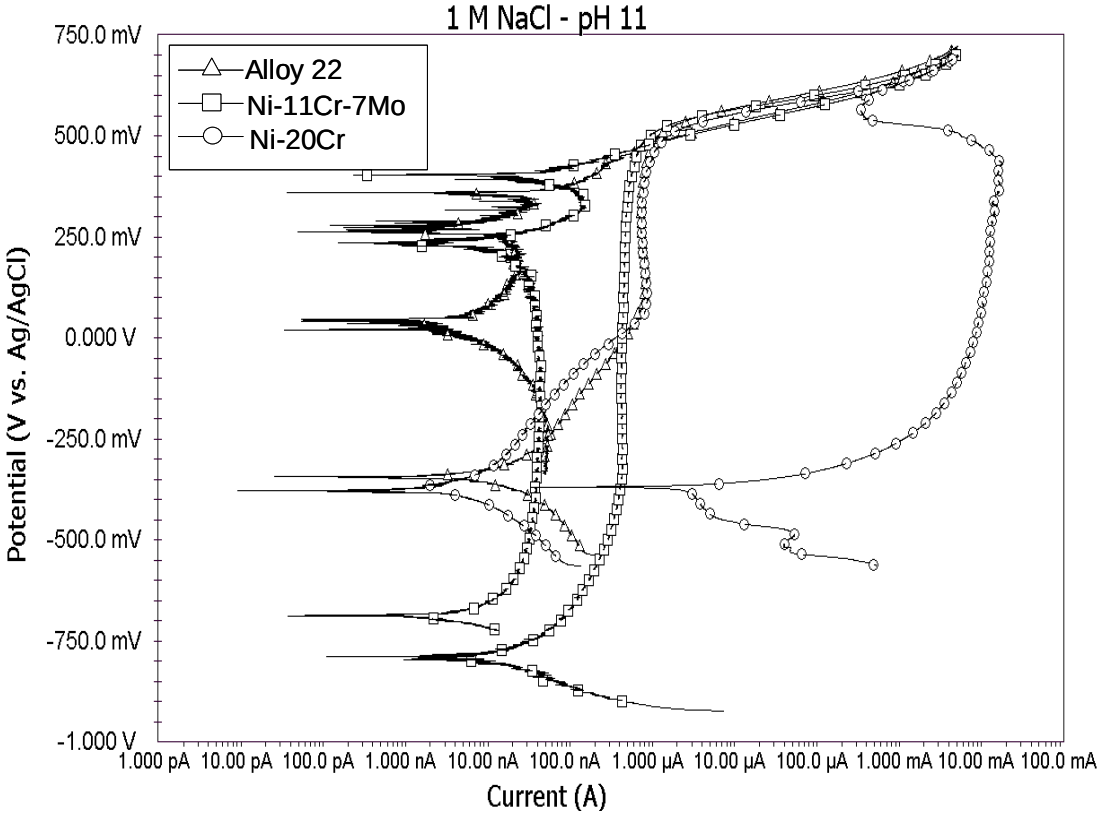

Figure 4: Cyclic potentiodynamic polarization of 3 alloys in 1 M NaCl solution at pH 11.

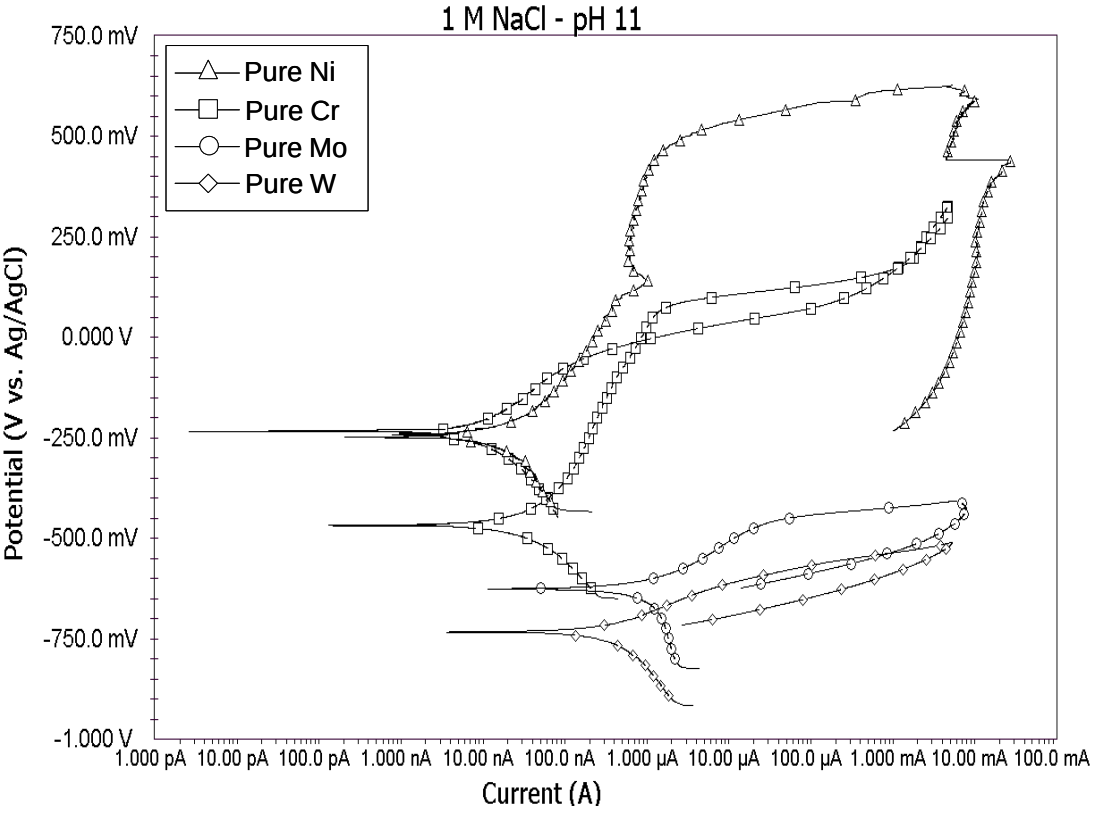

Figure 5: Cyclic potentiodynamic polarization of 4 pure metals in 1 M NaCl solution at pH 11.